33rd Annual International Conference of the IEEE EMBS
Boston, Massachusetts USA, August 30 - September 3, 2011

Statistical Model for Cardiovascular Signals with Independent Respiratory Modulation for Tracking Pulse Pressure Variation

James McNames, Sunghan Kim, and Mateo Aboy

Abstract— **Cardiovascular signals including the electrocardiogram, pressure signals, and photoplethysmographs such as those used in pulse oximetry contain a wealth of information. Statistical models of these signals provide a means of representing and quantifying this information, and often lead to natural and optimal estimation algorithms. One powerful statistical model uses a Fourier approach to model cardiovascular signals as a harmonic sum of sinusoids with a fundamental frequency, amplitudes, and phases that vary slowly over time. We have further developed this model to incorporate respiratory effects including an additive component, pulse pressure variation (PPV), and respiratory sinus arrhythmia. PPV may be viewed as a form of amplitude modulation of the cardiovascular signal due to respiration. Current models do not explain the asymmetry between the upper and lower envelopes observed in cardiovascular pressure signals, and consequently are not appropriate for PPV estimation. We propose a model in which each of the cardiac harmonics is independently modulated by the respiratory signal. This improves the estimation accuracy and permits more accurate cardiovascular tracking and estimation. The proposed model is more accurate in PPV estimation applications.**

I. Introduction

Statistical models of biomedical signals often form the core of signal processing algorithms for cardiovascular signals. They are also often used for algorithm validation since the parameter of interest may not be directly measurable in real signals and statistical models permit complete control of all the statistical parameters of interest [1]. These statistical models are particularly useful when they can be expressed in the form of a state-space model because many of the available state space tracking algorithms can then be applied to continuously estimate the parameters of interest from observed signals.

Cardiovascular signals such as pressure signals, photoplethysmographs (PPG), and electrocardiograms (ECG) are affected by both the cardiac and respiratory cycles. The interactions of these cycles are complex and challenging to model. One approach to modeling these cycles is to represent them as sums of sinusoids,

$$y_n = \sum_{k=1}^{N_\mathrm{h}} a_k \cos\left(k\theta_n + \phi_k\right) \tag{1}$$

where y_n is the observed cardiovascular signal, N_h is the number of harmonics, a_k is the amplitude of the k^{th} harmonic, θ_n is the instantaneous angle, and ϕ_k is the phase of the k^{th} harmonic. Fourier series representations are often used to model and characterize periodic signals. This is a compact representation of the signal in which the frequency, harmonic amplitudes, and harmonic phases completely characterize the signal. This can be generalized for the case where the frequency, amplitude, and phases are time-varying [2]. However, this model does not characterize the interaction of the respiratory and cardiac cycles.

The pulse pressure variation (PPV) describes changes in the amplitude of a cardiovascular pressure signal due to respiration. This effect is similar to amplitude modulation used in communication systems. A normalized index of PPV in patients receiving full mechanical ventilation is used clinically as a predictor of who will have a significant increase in cardiac output due to an infusion of fluid [3]–[7]. PPV is analogous to an asynchronous amplitude modulation of the cardiac component of cardiovascular signals [2], [8].

In the specific case of cardiovascular pressure signals, models have been proposed for arterial blood pressure (ABP) and intracranial pressure (ICP) signals. These statistical models typically model cardiovascular pressure signals as a sum of harmonically related sinusoids that are amplitude- and frequency-modulated by respiration. This type of model has been widely used in a variety of applications [8]–[11].

The major limitation of the ABP signal model based on amplitude and frequency modulation of the cardiac component by the respiratory signal is that it does not explain the asymmetry typically observed between the upper and lower envelopes in ABP signals. This fundamental ABP feature has not been previously explained or modeled. We propose a novel statistical signal model for ABP signals which takes into account the asymmetric upper and lower envelopes encountered in the ABP pulse pressure variation (PPV).

II. Methods

A. Notation

We have adopted the notation used in [12] with minor modification. We used boldface to denote random processes,

James McNames is director of the Biomedical Signal Processing Laboratory. He is also professor and chair of the Department of Electrical and Computer Engineering at Portland State University, Portland, Oregon, USA. Email: mcnames@pdx.edu (corresponding author).

Sunghan Kim is a member of the Neural Systems and Dynamics Laboratory at UCLA, Los Angeles, California, USA. Email: ksunghan@mednet.ucla.edu.

Mateo Aboy is a member of the Biomedical Signal Processing Laboratory. He is also professor and chair of the Department of Electrical Engineering and Renewable Energy at Oregon Institute of Technology, Portland, Oregon, USA. Email: mateoaboy@ieee.org.

This work was presented in part at the 2009 6th International Workshop on Biosignal Interpretation, Yale University, New Haven, CT. The proceedings of this conference were not published.

This work was partly supported by the Thrasher Research Fund.

normal face for deterministic parameters and functions, upper case letters for matrices, lower case letters for vectors and scalars, and subscripts for time indices.

B. State-Space Model

A typical nonlinear state-space model with additive noise can be expressed as,

$$\boldsymbol{x}_{n+1} = f(\boldsymbol{x}_n) + \boldsymbol{u}_n \tag{2}$$

$$\boldsymbol{y}_n = h(\boldsymbol{x}_n) + \boldsymbol{v}_n \tag{3}$$

where (2) is a process model, (3) is a measurement model, $f(\cdot)$ and $h(\cdot)$ nonlinear functions of the ℓ dimensional state $\boldsymbol{x}_n$, and $\boldsymbol{u}_n$ and $\boldsymbol{v}_n$ uncorrelated white noise with variances q and r. $\hat{\boldsymbol{x}}_{n|0:n}$ denotes a causal estimate of $\boldsymbol{x}_n$ given all previous measurements $\boldsymbol{y}_{0:n} = \{\boldsymbol{y}_0, \ldots, \boldsymbol{y}_n\}$.

C. Measurement Model

Previously the cardiac signal of the ABP signal was assumed to be amplitude-modulated by the respiratory modulation signal $\boldsymbol{m}_n$,

$$\boldsymbol{y}_n = \boldsymbol{s}_n + \boldsymbol{v}_n \tag{4}$$

$$\boldsymbol{s}_n = \sum_{k=1}^{N_\mathrm{h}^\mathrm{r}} \boldsymbol{r}_{1,k,n} \cos(k\boldsymbol{\theta}_n^\mathrm{r}) + \boldsymbol{r}_{2,k,n} \sin(k\boldsymbol{\theta}_n^\mathrm{r}) + \boldsymbol{m}_n \sum_{k=1}^{N_\mathrm{h}^\mathrm{c}} \boldsymbol{c}_{1,k,n} \cos(k\boldsymbol{\theta}_n^\mathrm{c}) + \boldsymbol{c}_{2,k,n} \sin(k\boldsymbol{\theta}_n^\mathrm{c}) \tag{5}$$

$$\boldsymbol{m}_n = 1 + \sum_{h=1}^{N_\mathrm{h}^\mathrm{r}} \boldsymbol{\lambda}_{1,h,n} \cos(h\boldsymbol{\theta}_n^\mathrm{r}) + \boldsymbol{\lambda}_{2,h,n} \sin(h\boldsymbol{\theta}_n^\mathrm{r}) \tag{6}$$

where N_h^r is the number of respiratory harmonics, N_h^c the number of cardiac harmonics, $\boldsymbol{\theta}_n^\mathrm{r}$ the instantaneous respiratory angle, $\boldsymbol{\theta}_n^\mathrm{c}$ the instantaneous cardiac angle, and $\boldsymbol{v}_n$ the measurement noise with variance r [2]. This cardiac signal is amplitude-modulated by the respiratory modulation signal $\boldsymbol{m}_n$. This model assumes that all harmonics of the cardiac signal are equally amplitude-modulated by $\boldsymbol{m}_n$.

We propose a new model for pressure signals that permits the respiratory signal to modulate each of the cardiac harmonics differently,

$$\boldsymbol{y}_n = \boldsymbol{s}_n + \boldsymbol{v}_n \tag{7}$$

$$\boldsymbol{s}_n = \sum_{k=1}^{N_\mathrm{h}^\mathrm{r}} \boldsymbol{r}_{1,k,n} \cos(k\boldsymbol{\theta}_n^\mathrm{r}) + \boldsymbol{r}_{2,k,n} \sin(k\boldsymbol{\theta}_n^\mathrm{r}) + \sum_{k=1}^{N_\mathrm{h}^\mathrm{c}} \boldsymbol{m}_{k,n} \left[\boldsymbol{c}_{1,k,n} \cos(k\boldsymbol{\theta}_n^\mathrm{c}) + \boldsymbol{c}_{2,k,n} \sin(k\boldsymbol{\theta}_n^\mathrm{c})\right] \tag{8}$$

$$\boldsymbol{m}_{k,n} = 1 + \sum_{h=1}^{N_\mathrm{h}^\mathrm{r}} \boldsymbol{\lambda}_{1,k,h,n} \cos(h\boldsymbol{\theta}_n^\mathrm{r}) + \boldsymbol{\lambda}_{2,k,h,n} \sin(h\boldsymbol{\theta}_n^\mathrm{r}) \tag{9}$$

In the new model each cardiac harmonic is separately amplitude-modulated by $\boldsymbol{m}_{k,n}$, where $\boldsymbol{m}_{k,n}$ is the respiratory modulation signal of the k^{th} cardiac harmonic.

D. Process Model

For the application of estimating the pulse pressure variation (PPV), patients must be under full ventilatory support. In this case, the respiratory rate is a known constant value. The process model for the instantaneous respiratory angle $\boldsymbol{\theta}_{n+1}^\mathrm{r}$ and instantaneous cardiac angle $\boldsymbol{\theta}_{n+1}^\mathrm{c}$ can then be written as,

$$\bar{\boldsymbol{f}}_{n+1}^\mathrm{c} = g\left[\bar{\boldsymbol{f}}_n^\mathrm{c} + \boldsymbol{u}_{\bar{\boldsymbol{f}}^\mathrm{c},n}\right] \tag{10}$$

$$\boldsymbol{f}_{n+1}^\mathrm{c} = \bar{\boldsymbol{f}}_n^\mathrm{c} + \alpha\left(\boldsymbol{f}_n^\mathrm{c} - \bar{\boldsymbol{f}}_n^\mathrm{c}\right) + \boldsymbol{u}_{\boldsymbol{f}^\mathrm{c},n} \tag{11}$$

$$\boldsymbol{\theta}_{n+1}^\mathrm{c} = \boldsymbol{\theta}_n^\mathrm{c} + 2\pi T_\mathrm{s} \boldsymbol{f}_n^\mathrm{c} \tag{12}$$

$$\boldsymbol{\theta}_{n+1}^\mathrm{r} = 2\pi(n+1) T_\mathrm{s} \boldsymbol{f}^\mathrm{r} \tag{13}$$

where T_s is the sampling period, $\boldsymbol{f}^\mathrm{r}$ a fixed respiratory rate, $\boldsymbol{f}_n^\mathrm{c}$ an instantaneous heart rate, α an autoregressive coefficient of $\boldsymbol{f}_n^\mathrm{c}$, and $\boldsymbol{u}_{\bar{\boldsymbol{f}}^\mathrm{c},n}$ and $\boldsymbol{u}_{\boldsymbol{f}^\mathrm{c},n}$ the process noises with variances $q_{\bar{\boldsymbol{f}}^\mathrm{c},n}$ and $q_{\boldsymbol{f}^\mathrm{c},n}$, respectively. The function $g[\cdot]$ is a nonlinear reflecting function,

$$g[f] = \begin{cases} f_{\max} - (f - f_{\max}) & f_{\max} < f \\ f & f_{\min} < f \leq f_{\max} \\ f_{\min} + (f_{\min} - f) & f \leq f_{\min}. \end{cases} \tag{14}$$

This essentially causes the mean frequency $\bar{\boldsymbol{f}}_n^\mathrm{c}$ to bounce elastically from the boundaries at $f_{\max}$ and $f_{\min}$, which in turn ensures that at any given time n the mean frequency $\bar{\boldsymbol{f}}^\mathrm{c}$ is uniformly distributed within this range.

The sinusoidal coefficients $\{\boldsymbol{r}_{1,k,n}, \ldots, \boldsymbol{\lambda}_{2,k,h,n}\}$ are modeled as random walk processes,

$$\boldsymbol{r}_{\cdot,k,n+1} = \boldsymbol{r}_{\cdot,k,n} + \boldsymbol{u}_{\boldsymbol{r},n} \tag{15}$$

$$\boldsymbol{c}_{\cdot,k,n+1} = \boldsymbol{c}_{\cdot,k,n} + \boldsymbol{u}_{\boldsymbol{c},n} \tag{16}$$

$$\boldsymbol{\lambda}_{\cdot,k,h,n+1} = \boldsymbol{\lambda}_{\cdot,k,h,n} + \boldsymbol{u}_{\boldsymbol{\lambda},n} \tag{17}$$

where $\boldsymbol{u}_{\boldsymbol{r},n}$, $\boldsymbol{u}_{\boldsymbol{c},n}$, and $\boldsymbol{u}_{\boldsymbol{\lambda},n}$ are white Gaussian process noises with variances $q_{\boldsymbol{r}}$, $q_{\boldsymbol{c}}$, and $q_{\boldsymbol{\lambda}}$, respectively. This process noise determine how quickly the sinusoidal coefficients are expected to change over time. The random walk is a common statistical model for parameters that are known to change slowly in time, but in which the exact dynamics of the changes are unknown [13].

E. Asymmetric Harmonic Envelopes

The new ABP signal model is motivated by our observation of the *asymmetric* upper and lower envelopes of ABP signals after removing the respiratory signal by applying a highpass filter. If the cardiac signal is amplitude-modulated by the respiratory modulation signal as shown in (5), the upper and lower envelopes of ABP signals after removing the respiratory signal should have the same amplitude modulation index, which indicates the *symmetric* amplitude modulation. However, often ABP signals do not exhibit symmetric amplitude modulation.

ABP signals included in this study are from the Massachusetts General Hospital (MGH) waveform database on PhysioNet, which is a comprehensive collection of electronic recordings of hemodynamic and electrocardiographic waveforms patients in critical care units [14]. The original sample

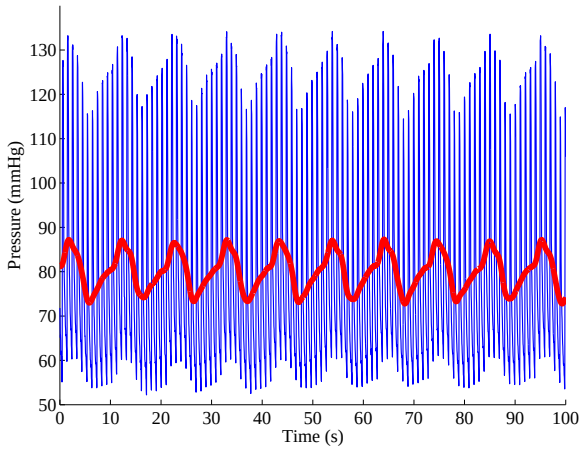

Fig. 1. ABP signal (blue) and its respiratory component (red).

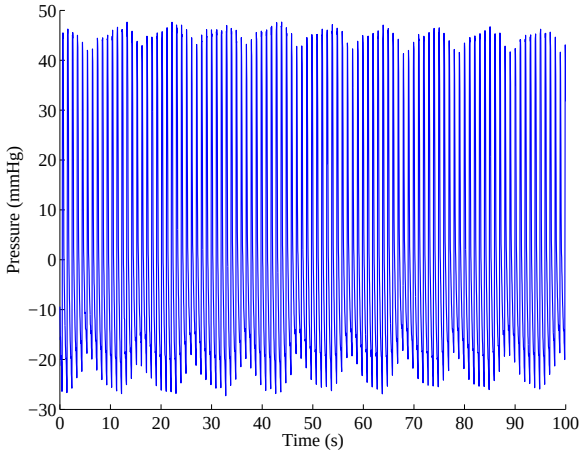

Fig. 2. Example of asymmetric amplitude modulation of the ABP signal, from which the respiratory component and mean were removed. The conventional ABP signal model can not model this asymmetry properly.

rate f_s of the signals was 360 Hz, but we downsampled them by a factor of 9 to a final sample rate of 40 Hz to reduce the computational load.

Fig. 1 shows an example of an ABP signal from the MGH database (blue) and its respiratory component (red). Fig. 2 illustrates the ABP signal after removing its respiratory component, $\boldsymbol{s}_n^{\text{-r}}$, which can be expressed as,

$$\boldsymbol{s}_n^{\text{-r}} = \boldsymbol{y}_n - \sum_{k=1}^{N_{\text{h}}^{\text{r}}} \boldsymbol{r}_{1,k,n} \cos\left(k\boldsymbol{\theta}_n^{\text{r}}\right) + \boldsymbol{r}_{2,k,n} \sin\left(k\boldsymbol{\theta}_n^{\text{r}}\right) \qquad (18)$$

The upper and lower envelopes of the signal $\boldsymbol{s}_n^{\text{-r}}$ shown in Fig. 2 exhibit asymmetric amplitude modulation. The observation of this asymmetric amplitude modulation led us to conclude that the conventional ABP signal model in (4)–(6) is incorrect.

In order to study the cause of this asymmetric amplitude modulation effect we applied three bandpass filters with different cutoff frequencies to the ABP signal shown

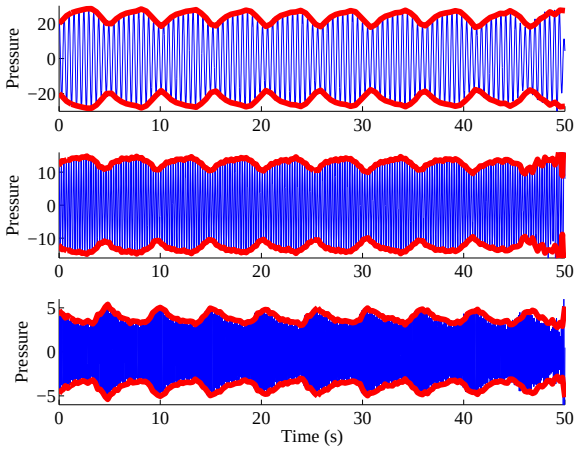

Fig. 3. Each cardiac harmonic partial along with its signal envelope. The envelopes of the third harmonic partial are out of phase from that of the first and second harmonic partials, which cannot be explained by the conventional ABP signal model.

in Fig. 2. Plots in Fig. 3 illustrate the resulting signals $\{\boldsymbol{b}_{1,n}, \boldsymbol{b}_{2,n}, \boldsymbol{b}_{3,n}\}$ (blue) and their upper and lower envelopes (red). According to the conventional ABP signal model shown in (4)–(6), the envelopes of $\{\boldsymbol{b}_{1,n}, \boldsymbol{b}_{2,n}, \boldsymbol{b}_{3,n}\}$ should be in-phase. However, Fig. 3 clearly indicates that the envelopes of $\boldsymbol{b}_{3,n}$ are out of phase from those of $\boldsymbol{b}_{1,n}$ and $\boldsymbol{b}_{2,n}$. This observation led us to propose the new ABP signal model in (7)–(9).

III. Results

An accurate statistical model is required to use state-space methods for continuous tracking of the parameters of interest. In order to demonstrate the suitability of the new ABP signal model, we developed two ABP signal trackers based on the conventional ABP signal model in (4)–(6) and the proposed one in (7)–(9) and applied them to the ABP signal shown in Fig. 1.

Previously we proposed a novel tracking algorithm which can compute the pulse pressure variation (PPV) of ABP signals continuously [15]. This algorithm can track the heart rate $\boldsymbol{f}_n^{\text{c}}$ along with the signal morphology represented by sinusoidal coefficients $\{\boldsymbol{r}_{\cdot,k,n}, \boldsymbol{c}_{\cdot,k,n}, \boldsymbol{\lambda}_{\cdot,k,h,n}\}$. We used this algorithm to implement two ABP trackers: one with the proposed state-space model and the other with the conventional one.

The top plot of Fig. 4 shows the 30 s segment (grey) of the ABP signal shown in Fig. 2. Estimates based on the proposed model (purple) and the conventional model (red) are shown along with their signal envelopes in the matching colors. The bottom plot of Fig. 4 illustrates the pulse pressure (PP) signals of the three ABP signals in the top plot. The pulse pressure signal is simply the difference between the ABP signal's upper and lower envelopes, which correspond to the systolic and diastolic pressures. The PP signal fluctuates approximately at the respiratory rate and the amplitude of its fluctuation (ΔPP) is referred to as the pulse pressure

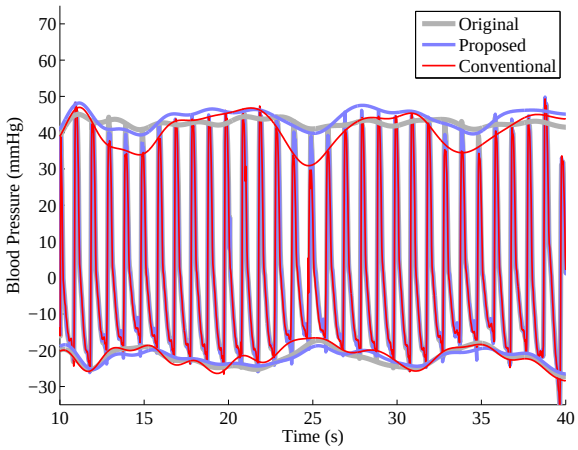

(a) ABP signals and their envelope estimates

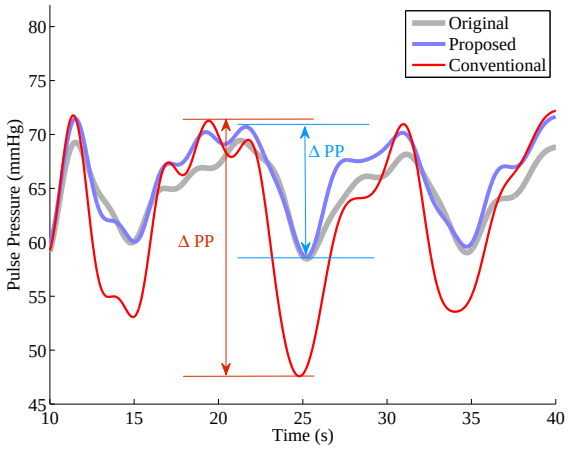

(b) Pulse pressure signals

Fig. 4. (a) ABP signals: original (grey), its estimates based on the proposed model (purple) and the conventional model (red). The corresponding signal envelopes in the matching colors (b) Pulse pressure (PP) signals of the original ABP signal (grey), its estimates based on the proposed model (purple) and the conventional model (red). ΔPP of the conventional model based result (red) overestimates the true ΔPP.

variation (PPV). It is a sensitive and yet specific predictor of fluid responsiveness in patients under full mechanical ventilation. ΔPP based on the conventional signal model overestimates the true ΔPP. In contrast, ΔPP based on the proposed signal model yields excellent results. This supports our claim that the proposed signal model more accurately represents the actual cardiovascular effects of respiration on the pulse pressure than the conventional one.

IV. Conclusion

Earlier signal models of cardiovascular pressure signals have accounted for the pulse pressure variation effects of respiration. However, until now, this effect was assumed to apply equally to all of the harmonics of the cardiac component. We have found that the extent of modulation differs for the cardiac harmonics and separate coefficients of modulation must be used for each of these harmonics. This results in a more accurate signal model that can improve the accuracy of cardiovascular parameter estimation when state-space tracking algorithms are applied. This could lead to more accurate prediction and monitoring of fluid responsiveness in critical care settings and ultimately improve patient outcome.

References

[1] J. P. Kaipio and P. A. Karjalainen, "Simulation of nonstationary EEG." *Biol Cybern*, vol. 76, no. 5, pp. 349–356, May 1997.

[2] J. McNames and M. Aboy, "Statistical modeling of cardiovascular signals and parameter estimation based on the extended kalman filter," *IEEE Transactions on Biomedical Engineering*, vol. 55, no. 1, pp. 119–129, Jan. 2008.

[3] F. Michard, S. Boussat, D. Chemla, N. Anguel, A. Mercat, Y. Lecarpentier, C. Richard, M. R. Pinsky, and J. L. Teboul, "Relation between respiratory changes in arterial pulse pressure and fluid responsiveness in septic patients with acute circulatory failure." *American Journal of Respiratory and Critical Care Medicine*, vol. 162, no. 1, pp. 134–8, Jul 2000.

[4] F. Michard, L. Ruscio, and J. L. Teboul, "Clinical prediction of fluid responsiveness in acute circulatory failure related to sepsis." *Intensive Care Medicine*, vol. 27, no. 7, p. 1238, Jul 2001.

[5] F. Michard and J.-L. Teboul, "Predicting fluid responsiveness in ICU patients: a critical analysis of the evidence." *Chest*, vol. 121, no. 6, pp. 2000–8, Jun 2002.

[6] A. Kramer, D. Zygun, H. Hawes, P. Easton, and A. Ferland, "Pulse pressure variation predicts fluid responsiveness following coronary artery bypass surgery." *Chest*, vol. 126, no. 5, pp. 1563–8, Nov 2004. [Online]. Available: http://dx.doi.org/10.1378/chest.126.5.1563

[7] C. K. Hofer, L. Furrer, S. Matter-Ensner, M. Maloigne, R. Klaghofer, M. Genoni, and A. Zollinger, "Volumetric preload measurement by thermodilution: a comparison with transoesophageal echocardiography." *Br J Anaesth*, vol. 94, no. 6, pp. 748–55, Jun 2005. [Online]. Available: http://dx.doi.org/10.1093/bja/aei123

[8] M. Aboy, J. McNames, T. Thong, C. Phillips, M. Ellenby, and B. Goldstein, "A novel algorithm to estimate the pulse pressure variation index," *IEEE Transactions on Biomedical Engineering*, vol. 51, pp. 2198–2203, 2004.

[9] M. Aboy, O. W. Mrquez, J. McNames, R. Hornero, T. Trong, and B. Goldstein, "Adaptive modeling and spectral estimation of nonstationary biomedical signals based on Kalman filtering." *IEEE Trans Biomed Eng*, vol. 52, no. 8, pp. 1485–1489, Aug 2005.

[10] M. Czosnyka, Z. Czosnyka, and J. D. Pickard, "Laboratory testing of the Spiegelberg brain pressure monitor: a technical report." *J Neurol Neurosurg Psychiatry*, vol. 63, no. 6, pp. 732–735, Dec 1997.

[11] R. Hornero, M. Aboy, D. Absolo, J. McNames, and B. Goldstein, "Interpretation of approximate entropy: analysis of intracranial pressure approximate entropy during acute intracranial hypertension." *IEEE Trans Biomed Eng*, vol. 52, no. 10, pp. 1671–1680, Oct 2005.

[12] O. Cappé, S. Godsill, and E. Moulines, "An overview of existing methods and recent advances in sequential Monte Carlo," in *Proceedings of the IEEE*, vol. 95, no. 5. IEEE-INST ELECTRICAL ELECTRONICS ENGINEERS INC, May 2007, pp. 899–924.

[13] S. Bittanti and S. M. Savaresi, "On the parameterization and design of an extended Kalman filter frequency tracker," *IEEE Transactions on Automatic Control*, vol. 45, no. 9, pp. 1718–1724, Sep 2000.

[14] A. L. Goldberger, L. A. N. Amaral, L. Glass, J. M. Hausdorff, P. C. Ivanov, R. G. Mark, J. E. Mietus, G. B. Moody, C.-K. Peng, and H. E. Stanley, "PhysioBank, PhysioToolkit, and PhysioNet: Components of a new research resource for complex physiologic signals," *Circulation*, vol. 101, no. 23, pp. e215–e220, Jun. 2000, circulation Electronic Pages: http://circ.ahajournals.org/cgi/content/full/101/23/e215.

[15] S. Kim, M. Aboy, and J. McNames, "Pulse pressure variation tracking using sequential monte carlo methods," *Biomedical Signal Processing and Control*, 2011, accepted in February 2011.